Effect of disorder on slow light velocity in optical slow-wave structures

Shayan Mookherjea and Andrew Oh

University of California, San Diego, Mail Code 0407, La Jolla, California 92093, USA

Received August 3, 2006; revised October 25, 2006; accepted October 27, 2006;
posted October 31, 2006 (Doc. ID 73779); published January 12, 2007

Slow-wave optical structures such as coupled photonic crystal cavities, coupled microresonators, and similar coupled-resonator optical waveguides are being proposed for slowing light because of the nature of their dispersion relationship. Since the group velocity becomes small, slow light and enhanced light–matter interaction may be observed at the edges of the waveguiding band. We derive a model of the effects of disorder on slow light in such structures, obtaining a relationship between the root-mean-square variation in the coupling coefficients and how slow the light is at the band edge. © 2007 Optical Society of America

OCIS codes: 260.2030, 230.7370, 230.5750.

Although several aspects of slow light have been studied recently, the effects of disorder on light velocity in slow-wave structures have not yet been investigated. Here, we derive a new quantitative relationship describing how slow light (near the band edge) is affected by random variations in the nearest-neighbor coupling coefficients.

The prototypical slow-wave optical waveguide structure that we analyze is that of the coupled-resonator optical waveguide (CROW). A CROW is formed by placing optical resonators in a linear (or a two–three-dimensional) array to guide light from one end of this chain to the other by photon hopping between adjacent resonators, i.e., the spatiotemporal overlap of the electromagnetic fields of the resonators.[1–4] A CROW is basically the optical equivalent of the periodically loaded waveguide in the microwave community.[5] CROWs have been fabricated as coupled microrings, photonic crystal defects, microspheres, superstructure gratings in fibers, etc. Usually 10–100 coupled resonators are sufficient to observe experimentally the effects of the CROW dispersion relationship.[6]

In slow-wave structures, CROWs, and similar waveguides consisting of cascaded identical unit cells, the field evolution can be described by a matrix equation,[7]

$$i\frac{\mathrm{d}}{\mathrm{d}t}\mathbf{u} = M\mathbf{u}, \qquad (1)$$

where $\mathbf{u}$ is the state vector (column vector) listing the time-dependent excitation coefficients of the resonators. M is the coupling matrix, where the diagonal elements represent the self-coupling frequency shift and the off-diagonal elements represent the coupling between neighboring resonators.

Eigensolutions of Eq. (1) have the time-evolution behavior $\mathbf{u} \sim \exp(i\omega t)$ and, therefore, are found by solving the determinantal equation $|M - \omega I| = 0$, where I is the unit matrix. The corresponding spatial part of each eigenmode is, in the tight-binding approximation,

$$|k\rangle \equiv \sum_{n=1}^{N} e^{-inkR}\mathbf{E}_{\mathrm{single}}(\mathbf{r} - nR\hat{\mathbf{z}}), \qquad (2)$$

i.e., a Bloch sum over the single-resonator fields $\mathbf{E}_{\mathrm{single}}(\mathbf{r})$.

We calculate the density of states, $\rho(\omega)$, which is defined such that $\rho(\omega)\,\mathrm{d}\omega$ is the number of eigenstates in a small neighborhood of frequencies around ω. Figure 1 shows the normalized density of states, $\hat{\rho}(\omega) \equiv \rho(\omega)/(Nm)$, corresponding to a CROW of $N = 512$ resonators, each with two modes ($m = 2$) that could model, for example, the cw and ccw modes of a microring. The inter-resonator coupling coefficients are chosen from the uniform (or alternatively, the Gaussian) random distribution, with the definition

$$\hat{\kappa} \sim \kappa + \delta\kappa U[-1/2, 1/2], \quad \text{(Uniform)}, \qquad (3a)$$

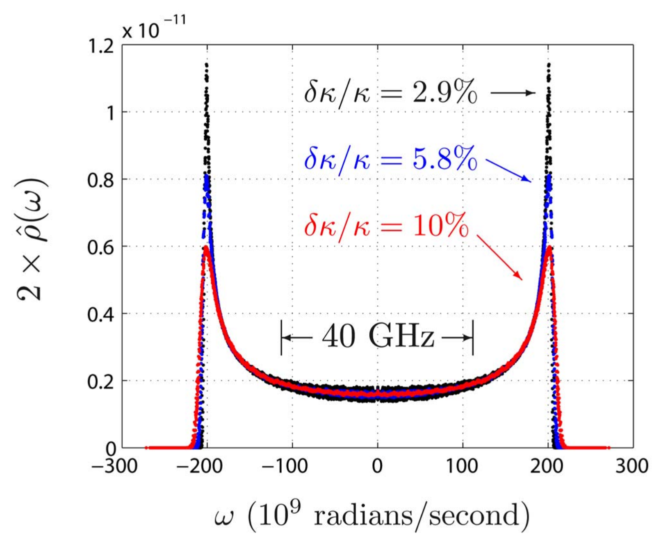

Fig. 1. (Color online) Density of states, $\hat{\rho}(\omega)$, obtained from a numerical calculation of the eigenvalues of the matrix M in Eq. (1). Indicated values of $\delta\kappa/\kappa$ represent the standard deviation in the coupling coefficients. The horizontal axis is the radian frequency detuning from the band center.

$$\hat{\kappa} \sim \kappa + \delta\kappa G[0;1], \quad \text{(Gaussian)}, \tag{3b}$$

where $\kappa = 100 \times 10^9$ rad/s, $U[-1/2, 1/2]$ is the uniform random distribution between $-1/2$ and $+1/2$, and $G[0;1]$ is the Gaussian random distribution with mean 0 and variance 1. 1024 Monte Carlo simulations are performed for each value of $\delta\kappa/\kappa$.

Figure 2 shows the numerically calculated dispersion relationship for weak disorder $\delta\kappa/\kappa = 3\%$ in the uniform random distribution. The dispersion relationship for the uniform tight-binding lattice and the disordered structure are practically coincident except near the band edge, which is shown in Fig. 2(b). We observe no isolated "islands" of disordered states beyond the tail of the spectrum, in agreement with Dean's earlier studies of glasslike lattices.[8]

Since $\rho(\omega)\mathrm{d}\omega = \rho(k)\mathrm{d}k$, our knowledge of $\rho(\omega)$ and $\rho(k)$ determines the group velocity, $v_g \equiv \mathrm{d}\omega/\mathrm{d}k = \rho(k)/\rho(\omega)$. At the band center, $\rho(\omega)$ takes its minimum value, and using $R = 10\ \mu\text{m}$ as an example for coupled microrings,

$$[v_g]_{\max} = \frac{1}{[\hat{\rho}(\omega)]_{\min}} \frac{1}{\pi/10\ \mu\text{m}} = 1.0 \times 10^6\ \text{m/s}. \tag{4}$$

This value agrees with that obtained directly from the dispersion relationship, $[v_g]_{\max} = (\delta\omega/2) \times R = 1 \times 10^6$ m/s, where $2\delta\omega$ is the full width of the passband ($2\delta\omega = 400 \times 10^9$ from Fig. 1). Note than approximately one order-of-magnitude reduction in $[v_g]_{\max}$ may be achieved by using coupled photonic crystal defect resonators instead of microrings.

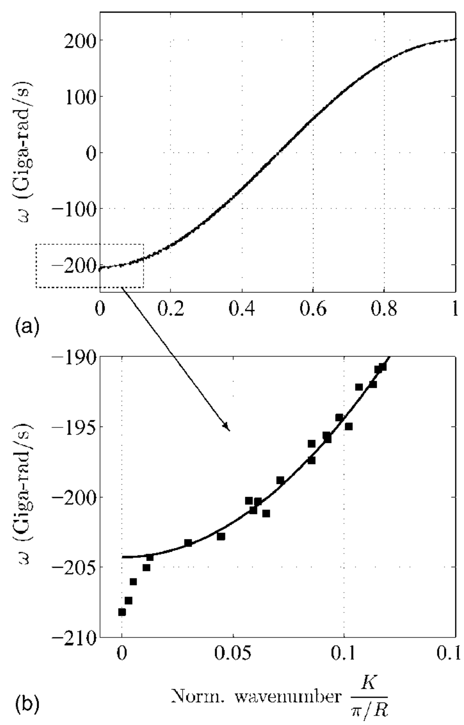

Fig. 2. Dispersion relationship of a weakly disordered optical tight-binding lattice for $\delta\kappa/\kappa = 3\%$ in the uniform random distribution is compared with the theoretical result (straight line). (a) The shape of the ideal dispersion curve, indicated by the solid curve, is reproduced over most of the range by the data points, except near the band edge, where as shown by (b), the slope in the disordered structure is not exactly zero and a tail extends into the bandgap region.

Now we turn our attention to the velocity of light in the disordered structure. Bearing in mind the conditions for its use as an optical delay line, we require of the structure that light be mostly transmitted through it in an "elastic" phase-coherent manner, i.e., in the ballistic transport regime. Indeed, both simulations[9,10] and experimental observations in the microwave regime[11] suggest that transmission is largely preserved in the presence of weak disorder, but the effect of disorder on the slow velocity of light was not directly measured or studied.

Change in $\rho(k)$: In the absence of disorder, the density of states in k-space is such that a total of $N \times m$ states are evenly distributed in the first Brillouin zone between $k = -\pi/R$ and $k = \pi/R$, i.e., $\rho_{\text{ideal}}(k) = Nm/(2\pi/R)$, where R is the inter-resonator spacing. In the presence of disorder, we represent by $\phi(k)$ the (average) phase shift induced over length $L = NR$ by the disorder at wavenumber k, so that

$$\phi(k) \sim \sum_{k'} (k - k')L \times (\text{number of states at } k') \times (\text{probability of transition: } k' \to k)$$
$$= \int \mathrm{d}k' (k - k') L \rho_{\text{ideal}}(k') W(k, k'), \tag{5}$$

where, from elementary scattering theory, $W(k, k') = |\langle k|\delta U(\mathbf{r})|k'\rangle|^2$, in terms of the spatial profile of the disorder, $\delta U(\mathbf{r})$.

From the resonance condition $kL + \phi(k) = 2m\pi$ for some integer m, we obtain

$$\rho(k) = \rho_{\text{ideal}}(k)\left(1 + \frac{1}{L}\frac{\mathrm{d}\phi}{\mathrm{d}k}\right). \tag{6}$$

For example, if we take $W(k, k') = W_0\delta(k - k') + W_1\delta(k + k')$, representing a scattering that has a "dc" component with amplitude W_0 and a frequency-conserving Bragg scattering term of amplitude W_1, then $\rho(k) = \rho_{\text{ideal}}(k)[1 + 2W_0\rho_{\text{ideal}}(k) + 2W_1\rho_{\text{ideal}}(-k)]$ is the new density of states in k-space.

Change in $\rho(\omega)$: In the absence of disorder, the density of states, $\rho(\omega)$, exhibits a divergence at the band edge, $\rho(\omega) \propto (\omega_{\text{edge}} - \omega)^{-1/2} \to \infty$ as $\omega \to \omega_{\text{edge}}$ and $v_g \to 0$. This is no longer true in the presence of disorder, as shown in Fig. 1. As the strength of disorder increases, $\hat{\rho}(\omega)$ and the dispersion relationship (Fig. 2) extend beyond precisely ±200 Grad/s. The density of states is redistributed within the available spectrum such that the integral over the density of states is constant. Thus, the peak value of $\hat{\rho}(\omega)$ is reduced.

We obtain the new $\rho(\omega)$ from results shown in Fig. 1 and similar numerical calculations. From the above discussion, we obtain the equation

$$v_g = \frac{1}{2\hat{\rho}(\omega)} \frac{1}{2\pi/R}\left(1 + \frac{1}{N}\frac{\mathrm{d}\phi}{R\mathrm{d}k}\right). \tag{7}$$

Figures 1 and 2 show that the group velocity in the tight-binding lattice is quite insensitive to weak disorder at the band center, and therefore, $[v_g]_{\max}$ is approximately equal to the value given in Eq. (4). The strongest effects of disorder are felt at the band edges, and we assume in this Letter, for simplicity, that $d\phi/dk$ can be neglected compared with the large changes in $\rho(\omega)$ in this narrow range of ω.

We calculate the band-edge slowing factor,

$$S_{\mathrm{be}} \equiv \frac{v_g \text{ at band center}}{v_g \text{ at band edge}}, \tag{8}$$

and plot S_{be} versus $\kappa/\delta\kappa$, as shown in Fig. 3. The numerically calculated data points lie almost exactly on a straight line fit (on a log–log scale):

$$\log_{10}(S_{\mathrm{be}}) = 0.644 \log_{10}\left(\frac{\kappa}{\delta\kappa}\right) + 0.272, \quad \text{(Uniform)}, \tag{9a}$$

$$\log_{10}(S_{\mathrm{be}}) = 0.648 \log_{10}\left(\frac{\kappa}{\delta\kappa}\right) + 0.281 - 0.648 \log_{10}\sqrt{12}, \quad \text{(Gaussian)}. \tag{9b}$$

The last factor on the right-hand side of Eq. (9b) represents the scaling of $\kappa/\delta\kappa$ to equate the variances in the two distributions, Eqs. (3a) and (3b).

To compare these observations with theoretical calculations, we refer to the investigations of Dyson[12] and Smith[13] calculating analytically the frequency spectrum of a disordered chain of coupled masses connected by elastic springs and of a linear chain of magnetic spins in an external field, respectively. The randomness in the coupling coefficients was modeled as a generalized Poisson distribution, which permits explicit analytical evaluation of $\hat{\rho}(\omega)$ [see Eqs. (4.6), (4.8), and (4.16) in Smith[13]] and leads to

$$\log_{10}(S_{\mathrm{be}})|_{\mathrm{theory}} = 0.667 \log_{10}(\kappa/\delta\kappa) + 0.313. \tag{10}$$

In view of the differences between a uniform random distribution and the generalized Poisson distribution, the agreement between Eqs. (9a) and (9b) and Eq. (10) is quite satisfactory, yielding the inference, $S_{\mathrm{be}} \sim (\kappa/\delta\kappa)^{2/3}$.

Thus, for variations in the inter-resonator coupling coefficients in the range of 1% to 10%, which covers the range of practical interest with current fabrication technology, slow light at the band edge is expected to be only 10 to 30 times slower than at the band center. This agrees with the experimentally measured values of this parameter, which are $S_{\mathrm{be}} \approx 7$ [optical regime; Ref. 14, Fig. 3(b)] and $S_{\mathrm{be}} \approx 6.5$ (microwave regime: Ref. 6, Fig. 4).[15]

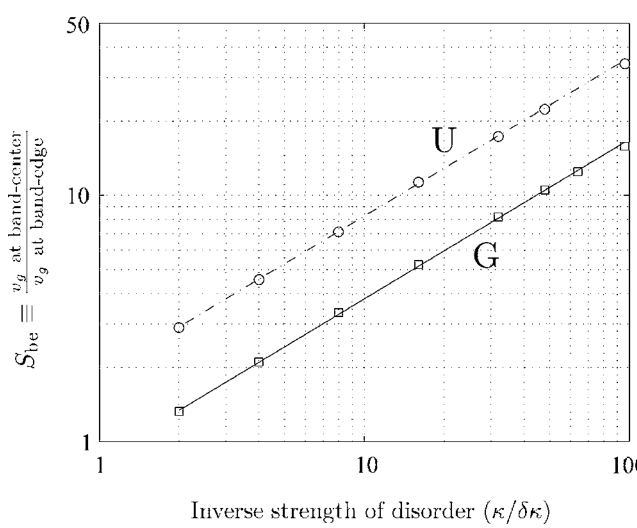

Fig. 3. Band-edge slowing factor obtained from numerical calculations of $\rho(\omega)$. The horizontal axis is the inverse strength of disorder, $(\delta\kappa/\kappa)^{-1}$, varying from 50% to 1%. U and G refer to the uniform and Gaussian random distributions in Eqs. (9a) and (9b), respectively. Those equations describe the straight-line best fit to the data points. The vertical distance between the lines is approximately $(2/3)\log_{10}\sqrt{12}$, to equate the variances of the two distributions.

The authors are grateful to the National Science Foundation for support and the San Diego Supercomputing Center for computational resources. E-mail: mookherjea@ece.ucsd.edu.

References

1. N. Stefanou and A. Modinos, Phys. Rev. B **57**, 12127 (1998).
2. A. Yariv, Y. Xu, R. K. Lee, and A. Scherer, Opt. Lett. **24**, 711 (1999).
3. G. Gutroff, M. Bayer, J. P. Reithmaier, A. Forchel, P. A. Knipp, and T. L. Reinecke, Phys. Rev. B **64**, 155313 (2001).
4. M. Ghulinyan, M. Galli, C. Toninelli, J. Bertolotti, S. Gottardo, F. Marabelli, D. S. Wiersma, L. Pavesi, and L. C. Andreani, Appl. Phys. Lett. **88**, 241103 (2006).
5. J. C. Slater, *Microwave Electronics* (Dover, 1969), Chap. VIII.
6. M. Bayindir, B. Temelkuran, and E. Ozbay, Phys. Rev. Lett. **84**, 2140 (2000).
7. S. Mookherjea, J. Opt. Soc. Am. B **23**, 1137 (2006).
8. P. Dean, Proc. Phys. Soc. London **84**, 727 (1964).
9. H. Matsuoka and R. Grobe, Phys. Rev. E **71**, 046606 (2005).
10. B. Z. Steinberg, A. Boag, and R. Lisitsin, J. Opt. Soc. Am. A **20**, 138 (2003).
11. M. Bayindir, E. Cubukcu, I. Bulu, T. Tut, E. Ozbay, and C. Soukoulis, Phys. Rev. B **64**, 195113 (2001).
12. F. J. Dyson, Phys. Rev. **92**, 1331 (1953).
13. E. R. Smith, J. Phys. C **3**, 1419 (1970).
14. J. K. S. Poon, L. Zhu, G. DeRose, and A. Yariv, Opt. Lett. **31**, 456 (2006).
15. In Ref. 6, the authors derived Fig. 4 (inset) by fitting the data points by a sum-of-cosines, which forces the slope at the band edge to zero, even if this seems not to be indicated by the measured data points. We extracted $S_{\mathrm{be}} \approx 6.5$ from the data points (open circles) shown in Fig. 4.